

GEOB 402 – Assignment 1

Local Air Quality Study – Prince George, BC, 2018

Introduction

The city of Prince George, located in Northern British Columbia, has a population of

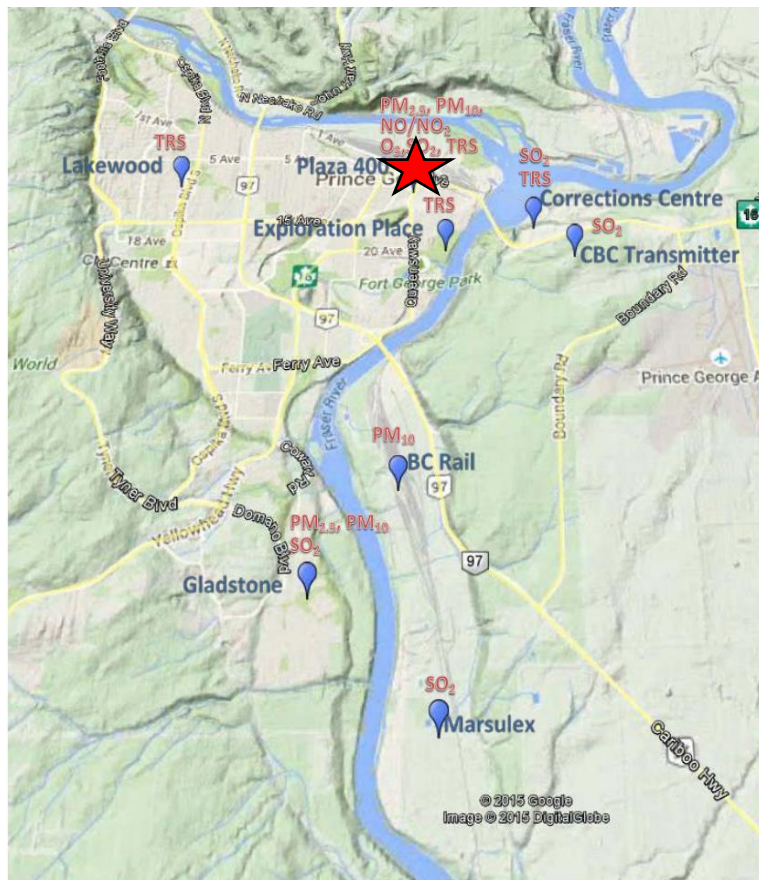


Figure 1: Map showing the locations and details of continuous air quality monitoring stations in Prince George. *Source:*

approximately 74,000 (BCStats, 2016) and is situated at the

confluence of the Nechako and

Fraser Rivers in a valley

approximately 150 meters below the

BC Central Interior Plateau (Fig. 1).

The city has gained notorious

reputation for poor air quality and

some of the highest pollutant levels

in BC. This study particularly looks

at the PM_{2.5} data gathered at Plaza

400 (marked as a red star in Fig. 1)

for the year of 2018. PM_{2.5} is the

fine particulate matter with particles

smaller than 2.5 microns and comes

mainly from combustion sources

such as industrial operations,

vehicles and wood burning smoke

but can also be a byproduct from

chemical reactions among

pollutants and components of the

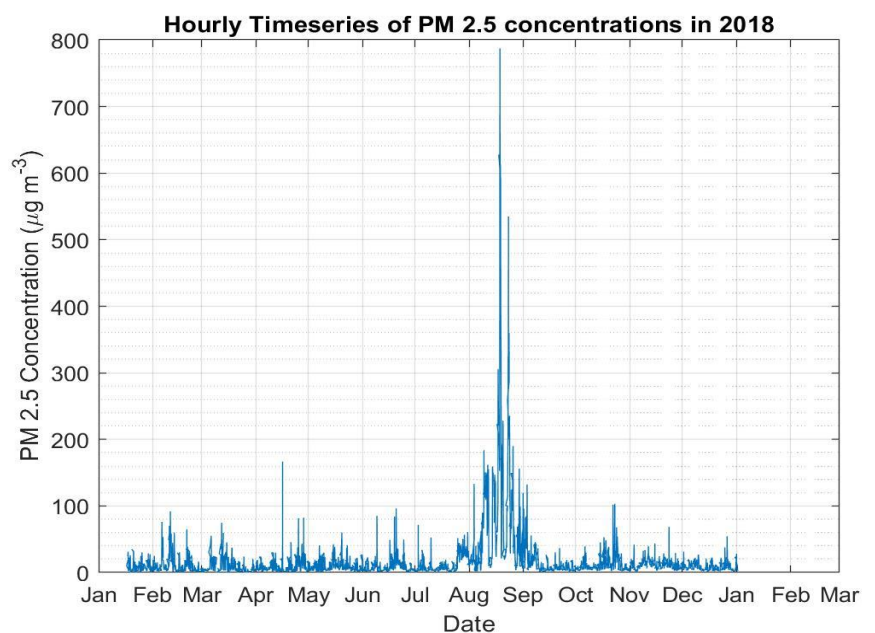
atmosphere. Natural sources include forest fires, windblown soil and dust, volcanic dust, sea spray, pollen, spores and bacteria. Anthropogenic sources of PM include fossil fuel combustion, industrial processes, prescribed burning, wood stoves, and fugitive dust from roads, construction sites and agriculture. (McKendry, 2006). Fine particulates pose significant threat to human health because their small size lets them deeply penetrate lung tissue, and in some cases even the bloodstream posing danger to lung and cardiac health.

Prince George's air quality problems can be hypothesized as a combination of meteorology, topography and land use. Approximately 44 industrial operations currently hold air emissions permits in and around Prince George which includes three pulp mills, an oil refinery, two asphalt plants, a host of sawmills, wood product plants and chemical operations (Simmons, 2007). Geographically the city is in a bowl-shaped valley, 450 km from the Pacific Ocean, and more than 500 km and 600 km, respectively, from the nearest major urban centers of Vancouver and Edmonton (Viera et al, 2013); making Prince George isolated from anthropogenic emission sources outside its own airshed. Additionally, atmospheric stagnation events due to anticyclonic conditions, thermal inversions and light winds in the valley often result in aggravated air conditions. Frequent summer-time forest fires in the province also degrade air quality in Prince George. This paper aims to detect and exemplify some of these instances from the diurnal and seasonal data acquired in 2018, discuss any anomalies, sources, sinks and exceedances in the scope of Prince George's PM_{2.5} concentration.

Data Acquisition and Observations:

The PM_{2.5} data and PM_{2.5} 24-hour running average data was acquired from the Air Quality Health Index (AQHI) data archive found on the BC Air Quality website. The data reported all PM_{2.5} concentrations in $\mu\text{g m}^{-3}$ and was compared with the Canada Wide Standard (CWS) for PM_{2.5} at $28 \mu\text{g m}^{-3}$ for a 24-hour running average to detect exceedances and their potential explanation.

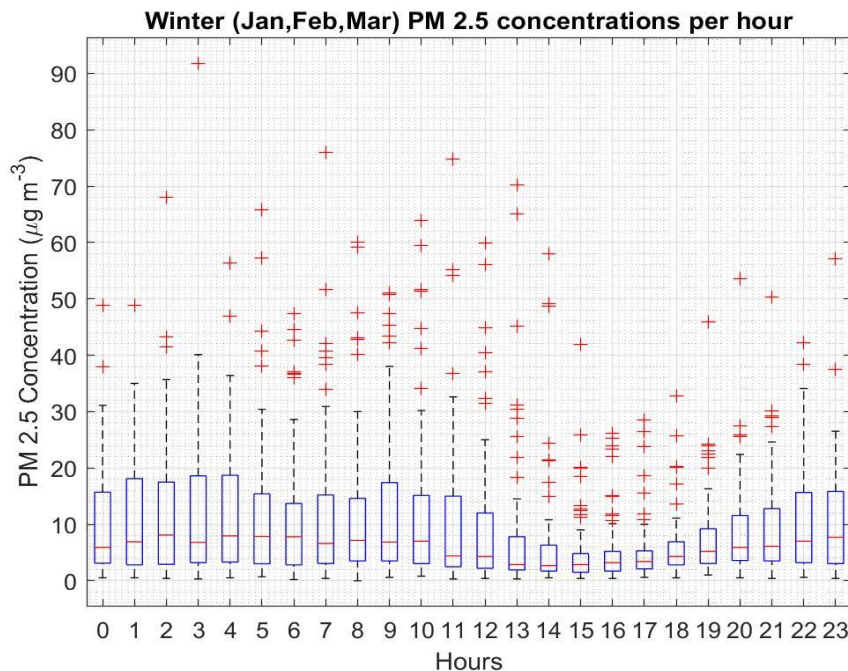
First the raw data was plot as a timeseries of PM_{2.5} concentration against time. As seen in Graph 1, there is a largely noticeable peak around the summer months, particularly mid-August to mid-September that reaches almost $630 \mu\text{g m}^{-3}$. Other noticeable peaks occur around April at $170 \mu\text{g m}^{-3}$ and others in February, June and October each around $100 \mu\text{g m}^{-3}$. Graph 1 alone does not provide a holistic view of the trend in PM_{2.5} and so further analysis was carried out by splitting the data into seasonal



Graph 1: Timeseries of hourly PM_{2.5} concentrations in 2018

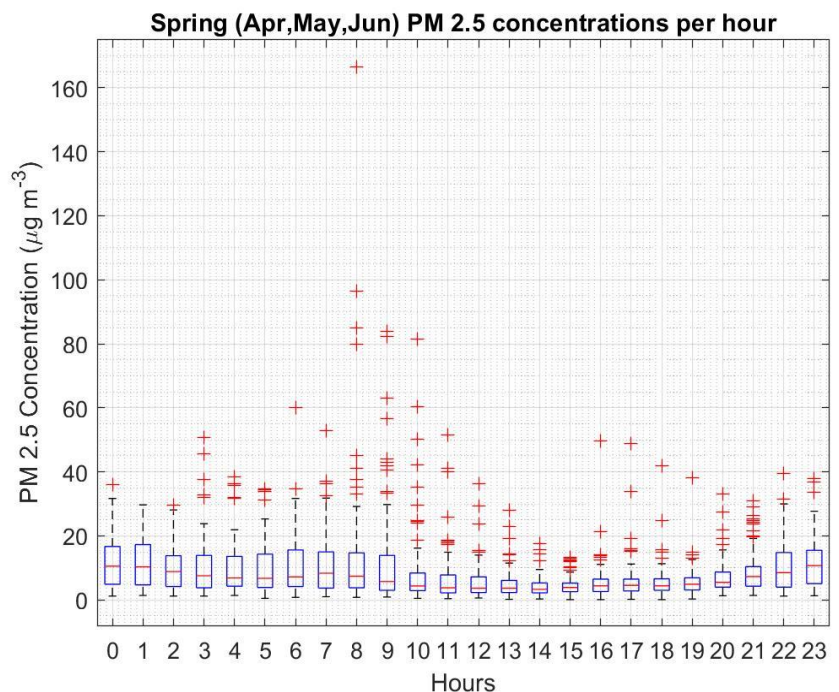
trends. Seasons are defined as the following:

- Winter- January, February, March
- Spring- April, May, June
- Summer- July, August, September
- Fall – October, November, December



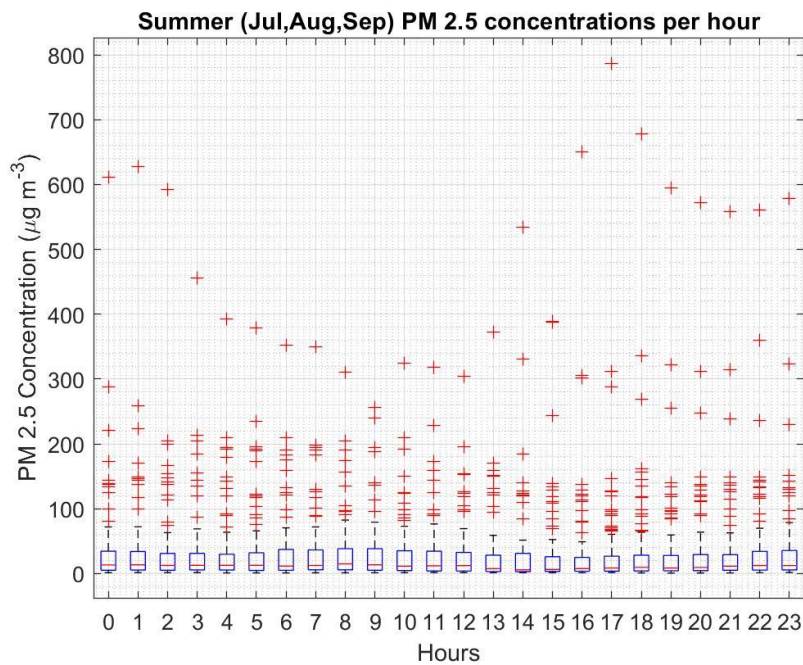
Graph 2: Diurnal distributions of PM_{2.5} concentration during winter 2018. Hour 0 starts at midnight.

number of outliers from all the however the diurnal variation is similar to the rest of the graphs. Highest concentrations of PM_{2.5} are seen during Spring and Summer. The concentrations are lower during fall and winter, with even outliers reaching a maximum of $100 \mu\text{g m}^{-3}$. In diurnal trends, from studying the medians we see that concentrations are usually lowest between noon to sunset and higher overnight. This trend is common to all the 4 seasons distinguished.

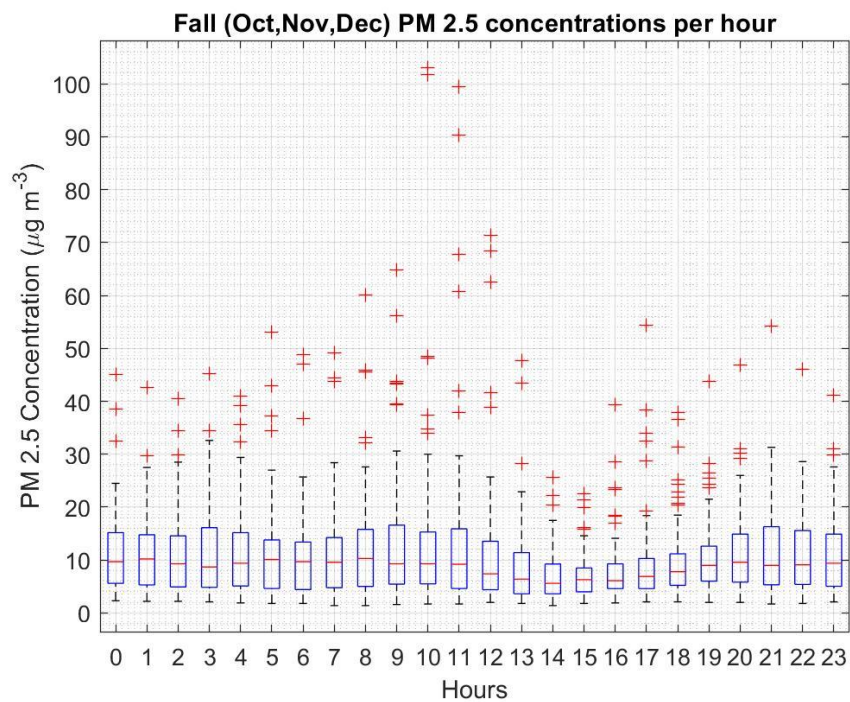


Graph 3: Diurnal distributions of PM_{2.5} concentrations during spring 2018. Hour 0 starts at midnight.

Graphs 2 through 5 below show the raw PM_{2.5} data split into 4 seasons and represented as boxplots that show the range of PM_{2.5} concentrations through the course of the day, for that season. As seen in Graphs 2 to 5, summer months have the highest

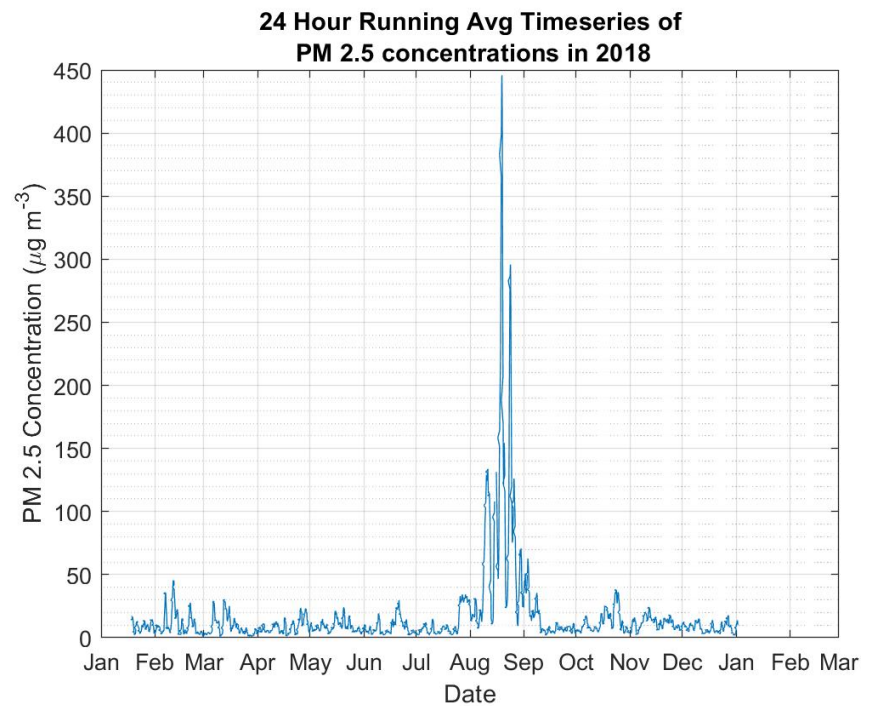


Graph 4: Diurnal distributions of PM_{2.5} concentrations during summer 2018. Hour 0 starts at midnight.

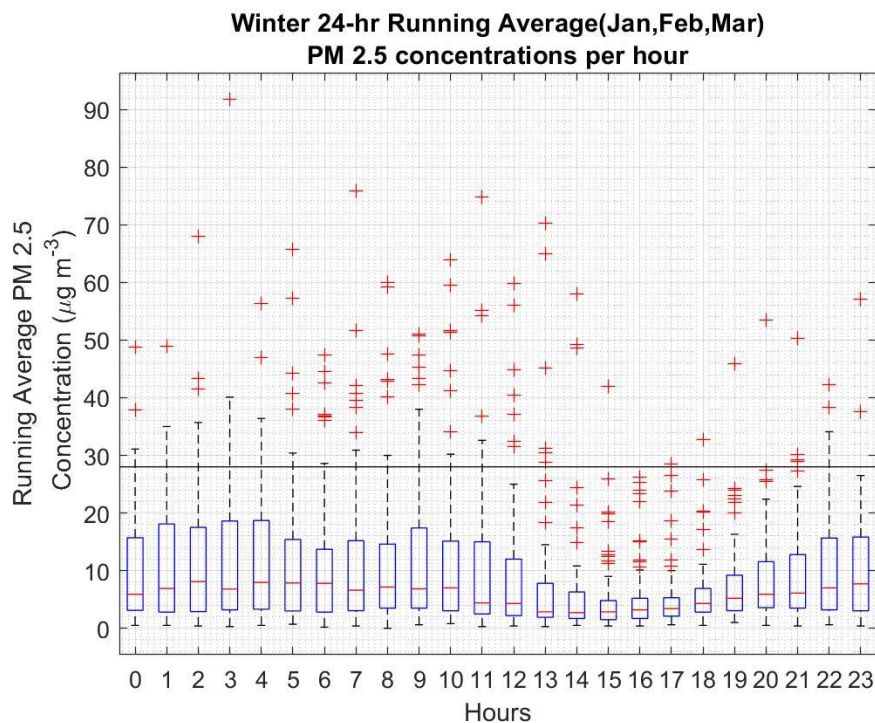


Graph 5: Diurnal distributions of PM_{2.5} concentrations during fall 2018. Hour 0 starts at midnight.

Similarly, an hourly timeseries and seasonal boxplots were also created for the 24-hour running average of the PM_{2.5} concentrations. The timeseries for this dataset is shown in Graph 6. The averaged data from Graph 6 has peaks at lower concentrations than seen in Graph 1. While the occurrence of these peaks aligns with the peaks from Graph 1, the largest peak occurs close to $450 \mu\text{g m}^{-3}$, while the others remain under $50 \mu\text{g m}^{-3}$. Graphs 7,8,9 and 10 are the diurnal boxplots split by season of the 24-hour running average of PM_{2.5}

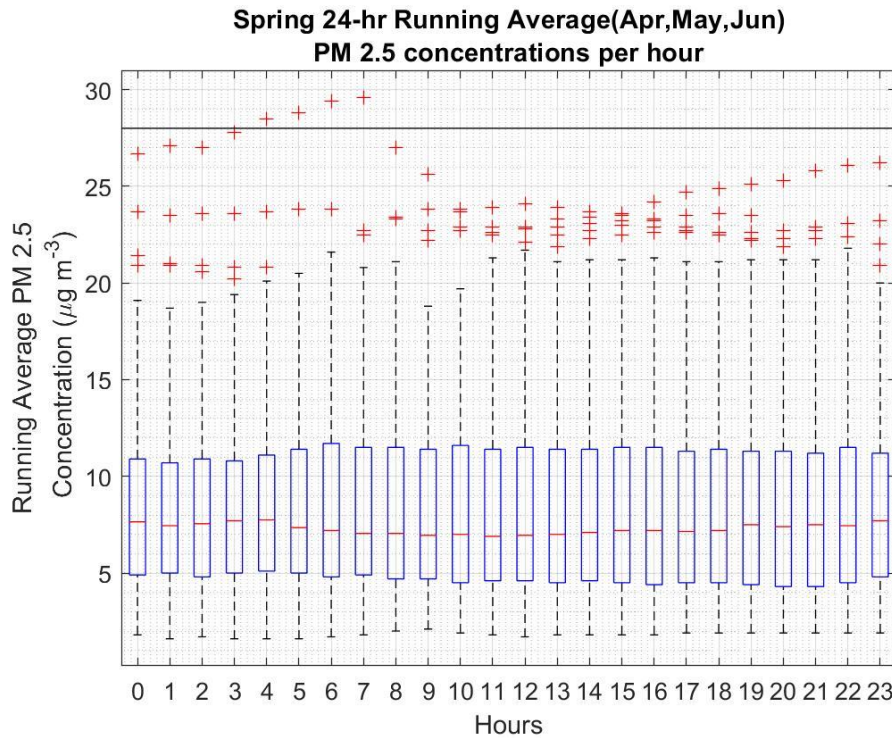


Graph 6: Timeseries for 24 hour running averages in PM_{2.5} concentrations per hour in 2018



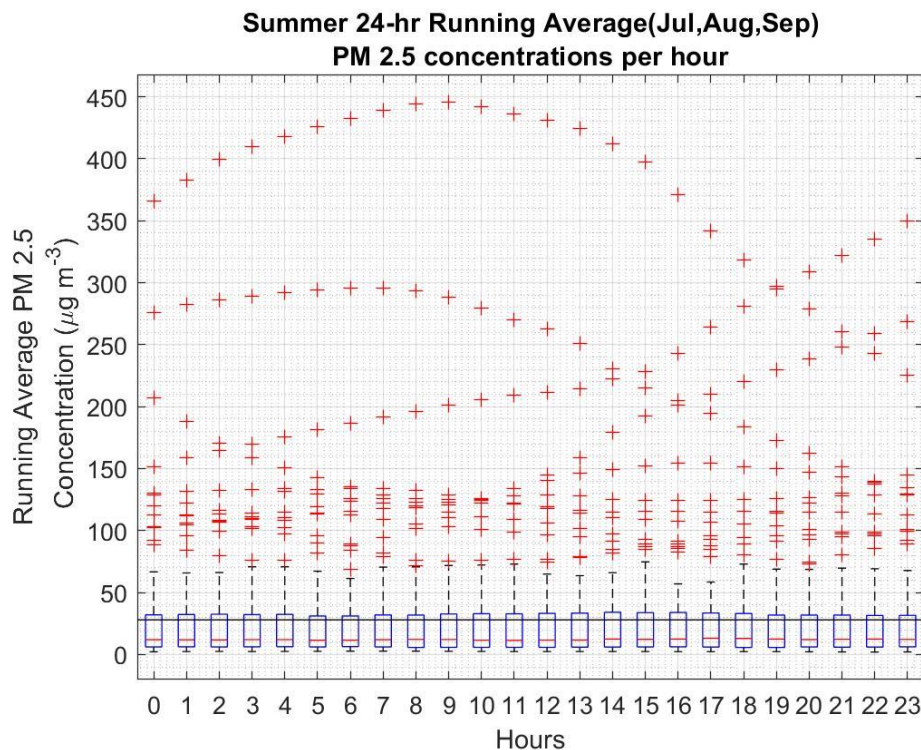
Graph 7: Diurnal distributions of 24 hour running averages of PM_{2.5} concentrations during winter 2018. Hour 0 starts at midnight.

concentrations as seen each hour. An additional line is added at $y = 28$ to mark the PM_{2.5} Canada Wide Standard of $28 \mu\text{g m}^{-3}$ (24 hour running average). The running average charts for spring and fall have their distributions all under the CWS for the diurnal pattern. Spring time concentrations do not fluctuate a lot, and the IQR remains similar across all the hours. There are very few outliers above the

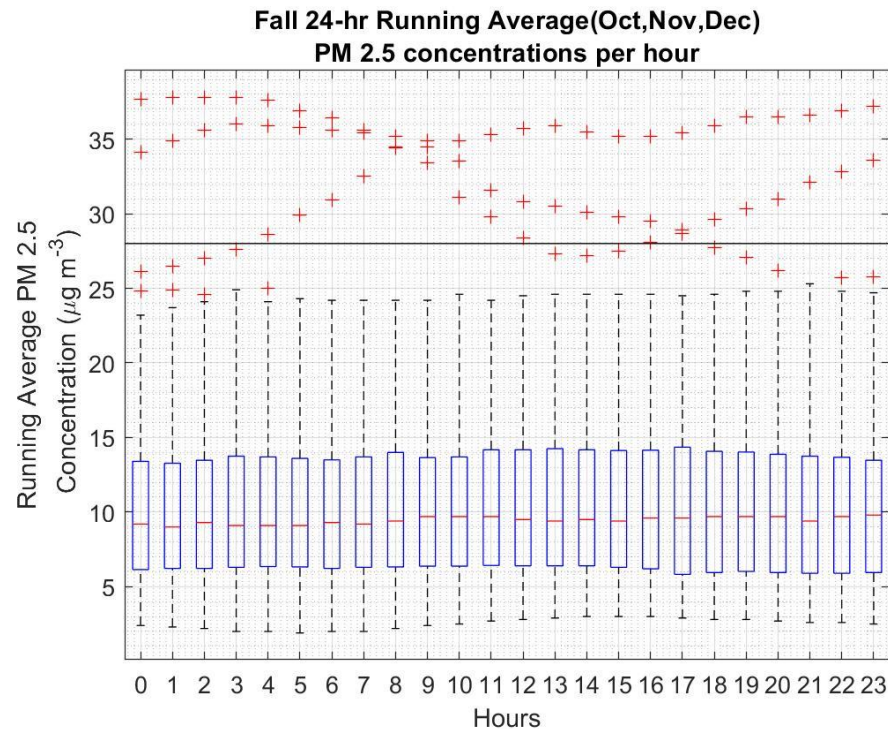


Graph 6: Diurnal distributions of 24 hour running averages of PM_{2.5} concentrations during spring 2018. Hour 0 starts at midnight.

CWS (Graph 8). The fall has more outliers above the CWS, but like in Spring, the IQR and median have very low variability (Graph 10). The winter plots have their 75% percentiles under the CWS in each hour, but higher variability in IQR and the median concentrations (Graph 7). The summer plots have the highest number of outliers and the CWS falls between the median and the 75% percentile for every hour. (Graph 8)



Graph 7: Diurnal distributions of 24 hour running averages of PM_{2.5} concentrations during summer 2018. Hour 0 starts at midnight.



Graph 8: Diurnal distributions of 24 hour running averages of PM_{2.5} concentrations during fall 2018. Hour 0 starts at midnight.

Discussion:

The observations made and data analyzed form a basis to research some of the sources and sinks that attribute to Prince George's air quality. The PG airshed topography can be looked upon as a plateau with a few hills surrounding the major rivers. The

Figure 2

topographic map shows the Tabor Mountain to the east, Cranbrook Hill to the west, and the Hart Highland area to the north. Figure 2 shows that the topography lowers appreciably at the intersection of the rivers resulting in a topographic "bowl" effect.

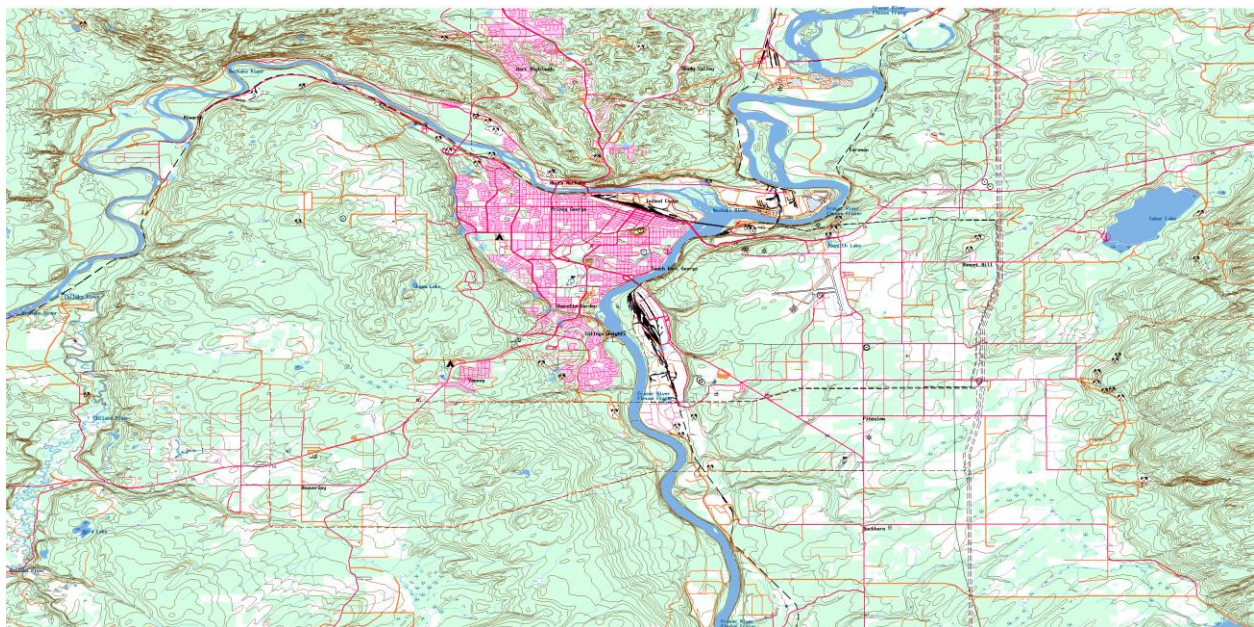


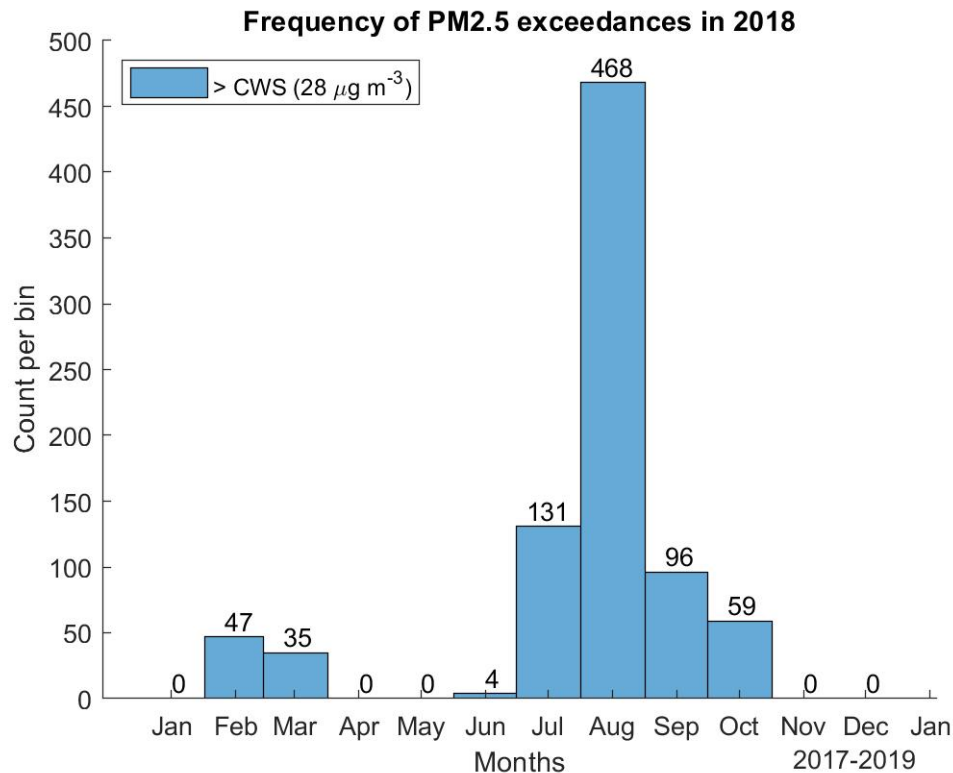
Figure 2: Topographic Map of Prince George. Source: canmaps.com

This wind sheltered valley experiences frequent temperature inversions when a stable, cold layer of air is overlain by warmer air as seen in the winter. Shallow (~100 m deep), surface-based inversions occur overnight due to surface cooling forming a stable nocturnal boundary layer which can explain the high PM concentrations seen overnight in Graphs 2,3,4 and 5. Deeper, elevated inversions that are more persistent occur due to subsidence associated with anticyclones. Winter meteorological conditions can create such anticyclones that can result in more frequent temperature inversions in the valley, less atmospheric mixing from daytime solar radiation reaching the surface, and consequently higher levels of PM_{2.5} pollution. We see this happen in Graphs 2 and 7 with their November and January peaks, but also in graphs 5,7 and 10 for the fall months, with higher variability in the median over the stretch of the day, larger Inter-Quartile Range (IQR) and even a greater fraction of hours with concentration reported above the CWS in the case of Graph 7. Winter snow cover will also result in less friction and so slower wind velocity, thereby decreasing the turbulence and creating light winds. These winds will remain over the airshed, creating persistent high PM_{2.5} concentrations in the bowl. Additionally two pulp mills and one oil refinery are less than 4 km northeast of Plaza and contribute significantly to ambient PM (both PM_{2.5} and PM₁₀) measured there especially when winds are from the northeast to southeast direction (Viera et. Al, 2013),. The valley winds and thermally forced winds due to valley heating create a subsidence in the valley and force the pollution upslope during the day, creating the lower concentrations observed in Graphs 2-5 between noon to sunset. These specifically occur after noon because the surface is heated enough after this point to create a thermal pressure gradient that drives these upslope winds. After sunset this pressure gradient no longer exists and the pollution pools back down into the valley overnight. As for land use and urban sources, colder temperatures also result in higher heating during the winter, as well as more people using cars and automobiles to get around and more wood burning fireplaces. All of these contribute to higher emissions and consequently higher concentrations of PM_{2.5}.

Spring on the other hand sees relatively lower PM_{2.5} concentrations. This is because these emissions are suppressed by rain and snow fall. Spring melt of a snowpack can suppress road-dust emissions and seasonal rainfall in both fall and spring also dilute the concentrations. Thus graph 8 and even 10 – although less so - on average remains under the CWS and has lower concentrations. They also see lower variability because often rain and high winds indicate more turbulence and thus a well-mixed airshed throughout the day.

However, a better understanding of the exceedances can be achieved from plotting them as a histogram, counting the number of exceedances each month. Note that the histogram is plotted

using the 24-hour running average data since the CWS of $28 \mu\text{g m}^{-3}$ is also reported as a 24-hour running mean for $\text{PM}_{2.5}$. Graph 11 shows this data.



Graph 9: Exceedances above CWS for $\text{PM}_{2.5}$ in 2018. Counts above each bin display the number of exceedances that month.

The $\text{PM}_{2.5}$ peaks most during the summer months. Graph 11 shows the frequency of $\text{PM}_{2.5}$ concentrations above the CWS of $28 \mu\text{g m}^{-3}$. As it can be seen in the graph, out of 840 exceedances in 2018, the majority of these (83%) occurred from

July-September (defined as summer in this study) as a result of wildfires, including the 91,253 hectare Shovel Lake Fire which ran upwind from Prince George, and Plaza 400. This peak in Graph 11 and Graphs 1 and 6, for dry summer conditions is primarily associated with forest fires and stagnation during anticyclonic periods resulting in fumigation events. The 2018 wildfire season was marked as the second worst in the province's history, with more than 12,984 square kilometers of the province being burned by the end of August. The remaining exceedances generally occurred during late winter periods when meteorological conditions can create stagnant conditions and wood burning appliances and other sources emit particulates that become trapped in the local air. Seasonal variations in $\text{PM}_{2.5}$ concentrations are evident in the time series of both Graph 1 and Graph 6. The plot identifies the summer exceedances linked to wildfires and the winter events linked to meteorological conditions. Most exceedances occurred between July and October with other exceedance events occurring in February and March. Overall the PG airshed sees more months with exceedances than not, but meteorology and seasonal events play a huge role in this pattern as opposed to just anthropogenic emission.

Bibliography

References

1. UPDATE: Shovel Lake wildfire held at 92,255 hectares [Internet].; 2018 [updated Sept 5,; cited Feb 13, 2019]. Available from: https://www.kelownanow.com/watercooler/news/news/Prince_George/BC_Wildfire_Service_responding_to_fire_near_Fraser_Lake/.
2. McKendry IG. Background Concentrations of PM2.5 and Ozone in British Columbia, Canada ; 2006 March.
3. Simmons MJ. The high price of bad air. 2007 Nov 19,.
4. Jackson PL, Albino J, Birch C, Nilson B, Pawluk J, Tereshchak T. Trends in fine particulate matter (PM2.5) concentrations in Prince George, British Columbia, Canada. 2017 Sept.
5. Jackson PL, Ainslie B, Fudge D. Assessment of background particulate matter concentrations in small cities and rural locations—Prince George, Canada AU - Veira, Andreas. Journal of the Air & Waste Management Association. 2013 July 1,;63(7):773-87.